Fluid level dependent Markov fluid model with continuous zero transition

Márton Balázs, Gábor Horváth, Sándor Kolumbán, Péter Kovács, Miklós Telek

Technical University of Budapest, 1521 Budapest, Hungary

Email: {balazs, kolumban, kpeter}@math.bme.hu, {ghorvath, telek}@hit.bme.hu

Abstract

Markov fluid models with fluid level dependent behaviour are considered in this paper. One of the main difficulties of the analysis of these models is to handle the case when in a given state the fluid rate changes sign from positive to negative at a given fluid level. We refer to this case as *zero transition*. The case when this sign change is due to a discontinuity of the fluid rate function results in probability mass at the given fluid level. We show that the case when the sign change is due to a continuous finite polynomial function of the fluid rate results in a qualitatively different behaviour: no probability mass develops and different stationary equations apply. We consider this latter case of sign change, present its stationary description and propose a numerical procedure for its evaluation.

Keywords: Markov fluid model, fluid level dependence, stationary behaviour, differential equation.

1 Introduction

Markov fluid model [13] is an efficient tool to describe stochastic system behaviour in a wide range of application fields. Examples of its application can be found in risk process modeling [3], in operation and maintenance modeling [4] and in modeling various telecommunication systems including e. g. congestion control of high-speed networks [8], traffic shapers for an on-off source [1] and single-wavelength optical buffers [12].

In the basic version of Markov fluid models [13] the fluid rates are independent of the fluid level. The numerically stable solution of these models requires a kind of eigenvalue separation. Two main ways are proposed for doing that. A purely algebraic method is proposed in [15] and a different thread of papers propose methods based on the stochastic interpretation of the fluid level process [2], [6].

In a more general set of Markov fluid models the fluid rates, as well as the transition rates of the governing

Markov chain, might depend on the fluid level but in a simple, piecewise constant way. The above mentioned solution methods are extended to the piecewise constant case in [11] and [7]. When the fluid rates and the transition rates are continuous, non-constant functions of the fluid level [5, 14] then the numerically stable methods based on eigenvalue separation are not applicable any more. A numerical solution method is proposed in [9] for the analysis of this case with the use of flux transition functions assuming that the fluid rate functions do not approach a predefined environment of zero. Here we do not consider the case when the transition rates of the governing Markov chain depend on the fluid level, we only note that the numerical solution of (15) is straightforward to extend to that case.

In this paper we consider the case when the fluid rate functions are allowed to cross zero level from positive rates to negative rates continuously according to a finite polynomial function. E.g., in a given state i the fluid rate function is $R_i(x) = 1 - 2x$ and the size of the fluid buffer is 1. In this case we say that this fluid rate function has a *continuous zero transition* (from positive fluid rate to negative one) at fluid level 1/2. Such a continuous zero transition results in qualitatively different behaviour at the fluid levels where the fluid rates change signs and consequently different stationary equations apply.

The case when the fluid rate function crosses the zero level from negative rates to positive ones is not particularly interesting and not discussed here. In that case there is no probability mass neither with discontinuous, nor with continuous zero transition and the method proposed below is applicable without any peculiar problem.

The rest of the paper is organized as follows. Section 2 briefly summarizes the background and Section 3 investigates the system behaviour at around the continuous zero transitions. Section 4 presents the proposed solution method. A numerical example is presented in Section 5 and the paper is concluded in Section 6.

2 Description of the system

The $Z(t) = \{M(t), X(t); t \geq 0\}$ process represents the state of a fluid model with single fluid buffer, where $M(t) \in \mathcal{S}$ is the (discrete) state of the environment process and $X(t) \in [0, B]$ is the fluid level of the fluid buffer at time t. $\mathcal{S}$ denotes the finite set of states of the environment and B denotes the maximum fluid level. The fluid level distribution might have probability masses at particular fluid levels and it is continuous between these levels. We define $\hat{\pi}_j(t, x)$ and $\hat{c}_j(t, x)$ to describe the transient fluid densities and the transient probability masses of the fluid distribution as follows

$$\hat{\pi}_j(t, x) = \lim_{\Delta \to 0} \frac{Pr(M(t) = j, x \leq X(t) < x + \Delta)}{\Delta} \ , \quad \hat{c}_j(t, x) = Pr(M(t) = j, X(t) = x) \ .$$

Assuming that the system converges to a unique stationary solution, the stationary fluid density function and fluid mass function are $\pi_j(x) = \lim_{t\to\infty} \hat{\pi}_j(t,x)$ and $c_j(x) = \lim_{t\to\infty} \hat{c}_j(t,x)$. On the continuous intervals of the fluid level distribution, row vector $\pi(x) = \{\pi_j(x)\}$, satisfies (see [10])

$$\frac{d}{dx}\Big(\pi(x)\mathbf{R}(x)\Big) = \pi(x)\mathbf{Q}(x) \ , \tag{1}$$

where matrix $\mathbf{Q}(x) = \{Q_{ij}(x)\}$ is the transition rate matrix of the environment process when the fluid level is x, and the diagonal matrix $\mathbf{R}(x) = \text{diag}\langle R_j(x)\rangle$ is composed by the fluid rates $R_j(x), j \in \mathcal{S}$. The fluid rate determines the rate at which the fluid level changes when the environment is in state j and the fluid level is x, i.e., $\frac{d}{dt}X(t) = R_j(x)$ when $X(t) = x$ and $M(t) = j$ and the transition rate matrix determines the rate at which discrete state transitions occur, i.e., $Q_{ij}(x) = \lim_{\Delta\searrow 0} Pr(M(t+\Delta) = j | M(t) = i, X(t) = x)/\Delta$ for $i \neq j$ and $Q_{ii}(x) = -\sum_{j\in\mathcal{S}, j\neq i} Q_{ij}(x)$, where $\searrow$ indicates that Δ converges to 0 from the right.

The stationary solution of the fluid model is characterized by the ordinary differential equation (ODE) (1). The main difficulty of finding the stationary solution is to find an appropriate set of boundary conditions for the ODE based on the stochastic behaviour of the fluid model. To the best of our knowledge such boundary conditions are not studied yet for Markov fluid models with continuous zero transition. The boundary conditions at fluid level 0 and B are [13, 9]:

$$-\pi_j(0)R_j(0) + \sum_k c_k(0)Q_{kj}(0) = 0 \ ,$$

$$\pi_j(B)R_j(B) + \sum_k c_k(B)Q_{kj}(B) = 0 \ ,$$

$$c_j(0) = 0 \ , \text{ if } R_j(0) > 0 \ , \quad c_j(B) = 0 \ . \text{ if } R_j(B) < 0 \ ,$$

The boundary conditions at the fluid levels of zero transitions require further considerations and are provided in the next section.

Following [9] we transform the system of equations by introducing the probability flux $\varphi_j(x)$,

$$\varphi_j(x) = \pi_j(x)R_j(x) \ . \tag{2}$$

Except the points of the zero transitions, with this notation (1) becomes

$$\frac{d}{dx}\varphi(x) = \varphi(x)\mathbf{R}^{-1}(x)\mathbf{Q}(x) \ , \tag{3}$$

where $\varphi(x)$ is a row vector, and the boundary conditions are

$$-\varphi_j(0) + \sum_k c_k(0) Q_{kj}(0) = 0 \ ,$$

$$\varphi_j(B) + \sum_k c_k(B) Q_{kj}(B) = 0 \ .$$

Model restrictions

To reduce notational and conceptual complexity in the rest of this paper we apply the following restrictions of the considered set of fluid models.

- The transition rate matrix is fluid level independent $\mathbf{Q}(x) = \mathbf{Q}$ and irreducible.
- The zero transitions are distinct, that is only one fluid rate tends to zero at each zero transition point.
- The fluid rates converge to non-zero limits at 0 and B.
- The zero transitions are from positive rates to negative ones.
- The diagonal elements of $\mathbf{R}(x)$ are bounded from below and from above by finite order continuous polynomial functions around the zero transitions.

The first restriction is easy to relax if $Q_{ij}(x) = 0$ or $|Q_{ij}(x)| > C$ for $\forall x \in [0, B]$ with positive constant C, i. e. the transition rates are either zero or non-zero and the non-zero ones never slow down to zero. The second restriction is also possible to relax but requires the introduction of a wide range of cumbersome cases, like linear zero transitions with different $-Q_{ii}/C_i$ ratio, or combination of linear and higher order zero transitions (see Section 3). The zero transitions from negative to positive fluid rates do not cause drift towards the point of zero transition and the model is solvable with the method presented in [9]. The last restriction is precisely formulated in the next theorem, and is rather important for the qualitative behaviour of the model. Relaxing this restriction might result in different qualitative behaviour (e.g. probability mass at zero transition). It is also possible to generalize the rate functions such that a combination of formerly studied cases (e. g. in [9]) and the zero transition of this paper coexist.

3 Properties at zero transition

We order the states such that the first $\hat{k}$ states ($1 < \hat{k} < n$) have negative rates in $[0, B]$, the states $\hat{k}+1, \hat{k}+2, \ldots, \hat{\ell} < n$ have zero transitions, and the last $n - \hat{\ell}$ states have positive rates in $[0, B]$.

Theorem 1. *Suppose*

- *for each* $j = 1, 2, \ldots, \hat{k}$, $R_j(x) < 0$, $x \in [0, B]$;

  for each $j = \hat{\ell} + 1, \hat{\ell} + 2, \ldots, n$, $R_j(x) > 0$, $x \in [0, B]$;

  there is a sequence of numbers $0 < x_{\hat{k}+1} < x_{\hat{k}+2} < \cdots < x_{\hat{\ell}} < B$ *such that for each* $j = \hat{k}+1, \hat{k}+2, \ldots, \hat{\ell}$, $R_j(x) > 0$ *if* $x < x_j$, $R_j(x_j) = 0$, *and* $R_j(x) < 0$, *if* $x > x_j$;

- *for each* $j = \hat{k} + 1, \hat{k} + 2, \ldots, \hat{\ell}$ *there are* $C_j, \tilde{C}_j > 0$, $\tilde{\alpha}_j \geq \alpha_j \geq 1$ *and* $1 > \delta_j > 0$ *constants such that if* $x \in (x_j - \delta_j, x_j + \delta_j)$,

$$\tilde{C}_j \cdot |x - x_j|^{\tilde{\alpha}_j} \leq |R_j(x)| \leq C_j \cdot |x - x_j|^{\alpha_j}, \tag{4}$$

  where

  * $\alpha_j = 1$ *and* $1 \leq \tilde{\alpha}_j < 1 + \min\left(1, \frac{-Q_{jj}}{C_j}\right)$, *or*
  * $\alpha_j > 1$ *and* $\alpha_j \leq \tilde{\alpha}_j < \alpha_j + 1$.

Then

a) there is no probability mass at x_j*'s and*

b) each probability flux $\varphi_j(x)$, $j = 1, 2, \ldots, n$ *stays bounded for* $x \in [0, B]$, $\varphi_j(x)$ *tends to* 0 *at* x_j *for* $j = \hat{k} + 1, \hat{k} + 2, \ldots, \hat{\ell}$.

c) Moreover, the density π_j *is bounded in an open neighborhood of* x_j *(*$\hat{k} + 1 < j \leq \hat{\ell}$*), if*

  * $\tilde{\alpha}_j = \alpha_j = 1$ *and* $-Q_{jj} > C_j$, *or*
  * $\tilde{\alpha}_j = \alpha_j > 1$.

Proof. The proof is composed by the following steps which are explained below. First we show that the flux is regular at x_i, $i = \hat{k} + 1, \hat{k} + 2, \ldots, \hat{\ell}$, then that the fluid density has a finite integral in the environment of x_i which, according to (1), implies that the probability flux tends to 0 and consequently that there is no probability mass at x_i, $i = \hat{k} + 1, \hat{k} + 2, \ldots, \hat{\ell}$.

Regularity of φ

According to (1) and (3) the stationary densities and fluxes satisfy

$$\sum_k \pi_k(x) Q_{ki} = \pi_i'(x) R_i(x) + \pi_i(x) R_i'(x), \tag{5}$$

and

$$\sum_k \varphi_k(x) \cdot \frac{Q_{ki}}{R_k(x)} = \varphi_i'(x), \qquad x \neq x_{\hat{k}+1}, x_{\hat{k}+2}, \ldots, x_{\hat{\ell}}. \tag{6}$$

Usual existence and uniqueness theorems cannot be applied to (5) at points x_i, while (6) is not even defined at these points. Due to $\mathbf{Q}$ being a Markovian generator ($\sum_i Q_{ki} = 0$), summing (6) over $i = 1, \ldots, n$ shows that

$$\sum_i \varphi_i'(x) = 0 \text{ and consequently } \quad \sum_i \varphi_i(x) = \text{constant}.$$

By stationarity this constant must be zero, that is

$$\sum_i \varphi_i(x) = 0. \tag{7}$$

We now fix $\hat{k} + 1 \leq j \leq \hat{\ell}$, and concentrate on $\varphi_j(x)$, the jth component of the solution as $x \searrow x_j$. Without loss of generality, we assume $x_j = 0$, and consider only $x \in (0, \min(\delta_j, x_{j+1}))$, so that for some $C > 0$,

$$\begin{gathered} R_1(x), \ldots, R_{j-1}(x) < -C, \qquad -C_j \cdot x^{\alpha_j} \leq R_j(x) \leq -\tilde{C}_j \cdot x^{\tilde{\alpha}_j} < 0, \\ C < R_{j+1}(x), \ldots, R_n(x). \end{gathered} \tag{8}$$

First we give an apriori bound which shows that the solution stays bounded everywhere. In the interval $x \in (0, \min(\delta_j, x_{j+1}))$, we sum (6) from 1 through j, and separate terms according to the signs of the rates:

$$\sum_{i=1}^{j} \varphi_i'(x) = \sum_{i=1}^{j} \sum_{k=1}^{j} \frac{Q_{ki}}{R_k(x)} \cdot \varphi_k(x) + \sum_{i=1}^{j} \sum_{\ell=j+1}^{n} \frac{Q_{\ell i}}{R_\ell(x)} \cdot \varphi_\ell(x). \tag{9}$$

Notice that $R_k(x)$ and $\varphi_k(x)$ have the same sign, and off-diagonal elements of Q are non-negative. Therefore the first term of the right hand side can be bounded as

$$\sum_{i=1}^{j} \sum_{k=1}^{j} \frac{Q_{ki}}{R_k(x)} \cdot \varphi_k(x) \leq \sum_{i=1}^{n} \sum_{k=1}^{j} \frac{Q_{ki}}{R_k(x)} \cdot \varphi_k(x) = 0,$$

where the last equality comes from $\sum_i Q_{ki} = 0$. Also, each term in the second sum of the right hand-side of (9) is non-negative, and by (8) we have

$$\frac{Q_{\ell i}}{R_\ell(x)} \leq D_1, \qquad i = 1, \ldots, j, \ \ell = j+1, \ldots, n$$

for some $D_1 > 0$. Hence we arrive to

$$\sum_{i=1}^{j} \varphi_i'(x) \le jD_1 \sum_{\ell=j+1}^{n} \varphi_\ell(x) = -jD_1 \sum_{\ell=1}^{j} \varphi_\ell(x),$$

where we used (7). Then by Grönwall's lemma $\sum_{i=1}^{j} \varphi_i(x)$ is bounded from below by the solution $y(x)$ of the Cauchy problem

$$y'(x) = -jD_1 \cdot y(x), \qquad y(\varepsilon) = \sum_{k=1}^{j} \varphi_k(\varepsilon),$$

on $(0,\, \varepsilon)$ for an $\varepsilon \in (0,\, \min(\delta_j,\, x_{j+1}))$. That is,

$$0 \ge \sum_{i=1}^{j} \varphi_i(x) \ge \sum_{k=1}^{j} \varphi_k(\varepsilon) \cdot \mathrm{e}^{jD_1(\varepsilon - x)}. \tag{10}$$

As approaching $x_j = 0$ from the right each term in the sum is non-positive, this shows boundedness of the terms. Via (7) and non-negativity, boundedness of the remaining $\varphi_{j+1}, \ldots, \varphi_n$ also follows.

The similar apriori bound as $x \nearrow x_{j+1}$ would work as follows: the second sum on the right hand-side of (9) is non-negative, hence

$$\begin{aligned}\sum_{i=1}^{j} \varphi_i'(x) &\ge \sum_{i=1}^{j}\sum_{k=1}^{j} \frac{Q_{ki}}{R_k(x)} \cdot \varphi_k(x) = -\sum_{i=j+1}^{n}\sum_{k=1}^{j} \frac{Q_{ki}}{R_k(x)} \cdot \varphi_k(x) \\ &\ge -(n-j)D_2 \sum_{i=1}^{j} \varphi_i(x),\end{aligned}$$

and Grönwall's lemma gives a bound very similar to (10).

Regularity of π

Now that we see boundedness of each $\varphi_k(x)$, we can turn back to (6):

$$\varphi_j'(x) = \frac{Q_{jj}}{R_j(x)} \cdot \varphi_j(x) + \sum_{k \ne j} \frac{Q_{kj}}{R_k(x)} \cdot \varphi_k(x).$$

With the already-proven boundedness of $\varphi_k(x)$, (8) and $x \in (0,\, \min(\delta_j,\, x_{j+1}))$, terms of the sum stay bounded, hence

$$\varphi_j'(x) \le \frac{-Q_{jj}}{C_j} x^{-\alpha_j} \varphi_j(x) + D_3, \tag{11}$$

where we used that $\varphi_j(x) < 0$, $Q_{jj} < 0$, $\alpha_j \geq 1$ and $0 < x < \min(\delta_j,\, x_{j+1}) < 1$. Again, Grönwall's inequality bounds $0 \geq \varphi_j(x)$ from below by the solution of

$$y'(x) = \frac{-Q_{jj}}{C_j} x^{-\alpha_j} y(x) + D_3, \qquad y(\varepsilon) = \varphi_j(\varepsilon). \tag{12}$$

For $\alpha_j = 1$ and $-Q_{jj} \neq C_j$ the closed-form solution is

$$y(x) = \Big(\varphi_j(\varepsilon)\varepsilon^{Q_{jj}/C_j} - \frac{D_3 C_j}{C_j + Q_{jj}} \varepsilon^{1+Q_{jj}/C_j}\Big) \cdot x^{-Q_{jj}/C_j} + \frac{D_3 C_j}{C_j + Q_{jj}} \cdot x,$$

while for $\alpha_j = 1$ and $-Q_{jj} = C_j$ we have

$$y(x) = \big(\varphi_j(\varepsilon)\varepsilon^{-1} - D_3 \ln \varepsilon\big) \cdot x + D_3 \cdot x \ln x.$$

Using (8) we arrive to

$$\begin{aligned} \pi_j(x) &= \frac{\varphi_j(x)}{R_j(x)} \leq \frac{-y(x)}{\tilde{C}_j \cdot x^{\tilde{\alpha}_j}} \qquad (13) \\ &= \begin{cases} \Big(\dfrac{D_3 C_j}{\tilde{C}_j(C_j + Q_{jj})} \varepsilon^{1+Q_{jj}/C_j} - \dfrac{\varphi_j(\varepsilon)}{\tilde{C}_j} \varepsilon^{Q_{jj}/C_j}\Big) \cdot x^{-Q_{jj}/C_j - \tilde{\alpha}_j} - \dfrac{D_3 C_j}{\tilde{C}_j(C_j + Q_{jj})} \cdot x^{1-\tilde{\alpha}_j} & \text{for } -Q_{jj} \neq C_j, \\ \Big(\dfrac{D_3}{\tilde{C}_j} \ln \varepsilon - \dfrac{\varphi_j(\varepsilon)}{\tilde{C}_j} \varepsilon^{-1}\Big) \cdot x^{1-\tilde{\alpha}_j} - \dfrac{D_3}{\tilde{C}_j} \cdot x^{1-\tilde{\alpha}_j} \ln x & \text{for } -Q_{jj} = C_j. \end{cases} \end{aligned}$$

We therefore see that, when $\alpha_j = 1$, the density is integrable if $1 \leq \tilde{\alpha}_j < 1 + \min\big(1,\, \frac{-Q_{jj}}{C_j}\big)$, and is bounded when $\tilde{\alpha}_j = 1 < \frac{-Q_{jj}}{C_j}$.

When $\alpha_j > 1$, a closed form solution of (12) is not available. Instead, we show that the solution is bounded from below by $4D_3 \frac{C_j}{Q_{jj}} \cdot x^{\alpha_j}$ for all small $x > 0$. Define $z(x) = x^{-\alpha_j} \cdot y(x)$, for this variable (12) becomes

$$z'(x) = \frac{-Q_{jj}}{C_j} x^{-\alpha_j} z(x) - \alpha_j x^{-1} z(x) + D_3 x^{-\alpha_j}, \qquad z(\varepsilon) = \varepsilon^{-\alpha_j} \cdot \varphi_j(\varepsilon).$$

Now suppose that z gets below $4D_3 \frac{C_j}{Q_{jj}}$ (recall that $Q_{jj} < 0$), and let

$$x^* = \min\Big[\sup\Big\{0 < x \leq \varepsilon \,:\, z(x) < 4D_3 \frac{C_j}{Q_{jj}}\Big\},\ \Big(\frac{-Q_{jj}}{2\alpha_j C_j}\Big)^{\frac{1}{\alpha_j - 1}}\Big].$$

Whenever in the interval $(0,\, x^*)$ we have $z(x) < 4D_3\frac{C_j}{Q_{jj}}$,

$$\begin{aligned} z'(x) &= \frac{-Q_{jj}}{2C_j}x^{-\alpha_j}\cdot z(x) + \Big(\frac{-Q_{jj}}{2C_j}x^{-\alpha_j} - \alpha_j x^{-1}\Big)\cdot z(x) + D_3 x^{-\alpha_j} \\ &\le \frac{-Q_{jj}}{2C_j}x^{-\alpha_j}\cdot z(x) + D_3 x^{-\alpha_j} \le -D_3 x^{-\alpha_j} \le 0. \end{aligned}$$

Thus we see that, in $(0,\, x^*)$, $z(x) \ge \min\big(4D_3\frac{C_j}{Q_{jj}},\ \varepsilon^{-\alpha_j}\cdot\varphi_j(\varepsilon)\big)$ holds from which

$$\pi_j(x) = \frac{\varphi_j(x)}{R_j(x)} \le \frac{-y(x)}{\tilde{C}_j\cdot x^{\tilde{\alpha}_j}} = x^{\alpha_j-\tilde{\alpha}_j}\cdot\frac{-z(x)}{\tilde{C}_j} \le x^{\alpha_j-\tilde{\alpha}_j}\cdot\max\Big(\frac{4D_3C_j}{-Q_{jj}\tilde{C}_j},\ \frac{\varepsilon^{-\alpha_j}\cdot(-\varphi_j(\varepsilon))}{\tilde{C}_j}\Big).$$

Integrability follows if $\tilde{\alpha}_j < \alpha_j + 1$, and we also see boundedness if $\tilde{\alpha}_j = \alpha_j$. □

4 Analysis of the stationary solution

4.1 Problems and proposed solutions

The main problem of the numerical solution of the system of differential equations (3) comes from the fact that these equations are singular at points $x_i,\quad i = \hat{k}+1,\dots,\hat{\ell}$, where the fluid rate crosses zero in one of the states. Since the system of equations cannot be evaluated in those points, the classical way of solving differential equations, i.e. marching from 0 to B in adequately small steps, does not work.

However, starting from a non-singular fluid level $x \in (x_i, x_{i+1})$, the flux can be computed based on (3) from x to the next singular fluid level x_{i+1}. Based on (3) we can also compute the flux from x to the previous singular fluid level x_i. Having these limitations we propose to compute the flux between two consecutive singular fluid levels staring from an internal point of the interval, e.g. from $x = (x_i + x_{i+1})/2$, and solving the differential equation forward and backward towards x_{i+1} and x_i.

To set up a system of equations between the flux vectors of the internal points of consecutive non-singular intervals e.g., $(x_{i-1}+x_i)/2$ and $(x_i+x_{i+1})/2$ and finally between fluid level 0 and B we propose the introduction of forward and backward flux transition matrices.

The forward and backward flux transition matrices can be computed in a similar way as the flux vector, i.e., if x is a non-singular point in (x_i, x_{i+1}) then the flux transition from x to $y \in [x_i, x_{i+1}]$ including $y \nearrow x_{i+1}$ and $y \searrow x_i$ can be computed. Therefore, the flux transition matrix between two arbitrary points can be expressed as the product of forward and backward flux transition matrices with non-singular starting points as it is discussed in the next subsection.

The second problem is associated with the numerical solution of (3) close to singularities.

Having the solution of (3) decomposed into consecutive non-singular intervals we still have the problem that the solution has bad numerical properties close to the singular fluid levels x_i, $i = \hat{k}+1, \ldots, \hat{\ell}$. Numerical differential equation solvers using fix step size cannot cope with this problem, and the procedures with automatic step size control experience intensive step size reduction as a singular fluid level is approached. To overcome this numerical problem we propose, in Section 4.4, a change of variable which results in a set of differential equations with bounded coefficients, whose solution has much better numerical properties.

4.2 Flux transition matrix

We define the forward and the backward *flux transition matrices* $\mathbf{V}(x, y)$ and $\mathbf{U}(y, x)$ $(x \leq y)$, respectively, such that

$$\varphi(y) = \varphi(x)\mathbf{V}(x, y), \quad \text{and} \quad \varphi(x) = \varphi(y)\mathbf{U}(y, x). \tag{14}$$

According to (3) $\mathbf{V}(x, y)$ and $\mathbf{U}(y, x)$ are the solution of

$$\frac{\partial}{\partial y}\mathbf{V}(x, y) = \mathbf{V}(x, y)\left(\mathbf{R}(y)^{-1}\mathbf{Q}\right) \quad \text{and} \quad \frac{\partial}{\partial x}\mathbf{U}(y, x) = \mathbf{U}(y, x)\left(\mathbf{R}(x)^{-1}\mathbf{Q}\right), \tag{15}$$

with initial value $\mathbf{V}(x, x) = \mathbf{U}(y, y) = \mathbf{I}$, where $\mathbf{I}$ is the identity matrix.

4.3 Solution of the system of equations

Let us define a set of non-singular points (levels of fluid) y_i, $i = \hat{k}, \ldots, \hat{\ell}$ as follows:

$$y_i = \begin{cases} 0, & i = \hat{k}, \\ \frac{x_i + x_{i+1}}{2}, & \hat{k} < i < \hat{\ell}, \\ B, & i = \hat{\ell}, \end{cases} \tag{16}$$

thus, each regime bounded by a boundary point or a zero crossing contains exactly one y_i.

Our aim is to obtain the fluid flux at points y_i, since the flux at an arbitrary point can be calculated based on them either with the forward or the backward flux transition function as

$$\varphi(x) = \begin{cases} \varphi(y_i)\mathbf{U}(y_i, x) & x_i \leq x \leq y_i, \\ \varphi(y_i)\mathbf{V}(y_i, x) & y_i \leq x \leq x_{i+1}. \end{cases} \tag{17}$$

We introduce the notation $K = \hat{\ell} - \hat{k}$, the number of fluid rates with zero transitions. For the unknowns

$\varphi(y_i)$, $i = \hat{k}, \ldots, \hat{\ell}$ we have the following set of linear equations.

1. Exploiting that at x_i we have $\varphi(x_i^-) = \varphi(x_i^+)$ gives

$$\varphi(y_{i-1})\mathbf{V}(y_{i-1}, x_i) = \varphi(y_i)\mathbf{U}(y_i, x_i). \tag{18}$$

   The continuity of $\varphi(x)$ at x_i follows from the fact that the integral of (1) from $x_i - \Delta$ to $x_i + \Delta$ tends to 0 as $\Delta \searrow 0$, because there is no probability mass at x_i. Since column i of $\mathbf{V}(y_i, x_i)$ and $\mathbf{U}(y_{i+1}, x_i)$ are zero because $\varphi_i(x) \to 0$ when $x \to x_i$, the linear system of (18) has $n-1$ non-trivial equations, thus all equations for $i = \hat{k}+1, \ldots, \hat{\ell}$ give a total number of $Kn - K$ non-trivial equations.

2. Let $c^-(x)$ ($c^+(x)$) and $\varphi^-(x)$ ($\varphi^+(x)$) be the vector composed by elements $c_i(x)$ and $\varphi_i(x)$ with negative (positive) rates at fluid level x, $R_i(x) < 0$ ($R_i(x) > 0$). Applying this fluid level dependent state partitioning based on the sign of the fluid rates the boundary conditions can be rewritten as

$$\varphi^-(0) = c^-(0)\mathbf{Q}^{--} , \tag{19}$$

$$c^+(0) = 0, \tag{20}$$

$$-\varphi^+(B) = c^+(B)\mathbf{Q}^{++} , \tag{21}$$

$$c^-(B) = 0, \tag{22}$$

$$\varphi^+(0) = c^-(0)\mathbf{Q}^{-+} , \tag{23}$$

$$-\varphi^-(B) = c^+(B)\mathbf{Q}^{+-} , \tag{24}$$

   that and some algebraic manipulations provide the following linear equations for $\varphi(0)$ and $\varphi(B)$:

$$\varphi^+(0) = \varphi^-(0)(-\mathbf{Q}^{--})^{-1}\mathbf{Q}^{-+}, \tag{25}$$

$$\varphi^-(B) = \varphi^+(B)(-\mathbf{Q}^{++})^{-1}\mathbf{Q}^{+-}. \tag{26}$$

   The number of equations in (25) and (26) is $(n - \hat{k}) + \hat{\ell}$ (number of positive rates at 0 and number of negative rates at B).

Since $(n - \hat{k}) + \hat{\ell} = n + K$, (18), (25) and (26) contain a total number of $(K+1)n$ non-trivial equations, that equals the number of unknowns. The solution of the linear system (18), (25) and (26) is subject to a constant multiplication. To make the solution unique we need to normalize it. To this end we compute the total probability of the stationary solution. It is the integral of the fluid densities plus the probability masses

at 0 and B,

$$\sum_{k=\hat{k}+1}^{\hat{\ell}} \left(\varphi(y_{k-1}) \int_{x=y_{k-1}}^{x_k} \mathbf{V}(y_{k-1},x)\mathbf{R}^{-1}(x)\mathbb{1}dx + \varphi(y_k) \int_{x=x_k}^{y_k} \mathbf{U}(y_k,x)\mathbf{R}^{-1}(x)\mathbb{1}dx \right) + c^-(0)\mathbb{1} + c^+(B)\mathbb{1}, \tag{27}$$

which should equal to 1.

4.4 Efficient computation of the flux transition matrices

Numerical solution of (15) from y_{k-1} to x_k (forward) and from y_k to x_k (backward) requires adaptive step size control at around x_k, because $R_k^{-1}(x)$ tends to infinity at $x = x_k$. The numerical properties of this solution method can be improved with an appropriate change of variable.

For the analysis of $\varphi_{\hat{k}+1}(x)$ in the interval $x \in [y_{\hat{k}} = 0, x_{\hat{k}+1}]$ we introduce

$$u = \int_{y=0}^{x} R_{\hat{k}+1}^{-1}(y)dy \tag{28}$$

and $k^* = \hat{k} + 1$. According to (28) u is a function of x, but to avoid notational confusion with the inverse of this function, denoted as $x(u)$, we do not indicate this dependence explicitly. (28) results in $du/dx = R_{k^*}^{-1}(x)$. Substituting these into (6) gives

$$\frac{du}{dx}\frac{d}{du}\varphi_i(x(u)) = \varphi_{k^*}(x(u)) \cdot \frac{Q_{k^*i}}{R_{k^*}(x(u))} + \sum_{k,k\neq k^*} \varphi_k(x(u)) \cdot \frac{Q_{ki}}{R_k(x(u))},$$

and

$$\frac{d}{du}\hat{\varphi}_i(u) = \hat{\varphi}_{k^*}(u) \cdot Q_{k^*i} + \sum_{k,k\neq k^*} \hat{\varphi}_k(u) \cdot \frac{\hat{R}_{k^*}(u)}{\hat{R}_k(u)} Q_{ki},$$

where $\hat{\varphi}_i(u) = \varphi_i(x(u))$, $\hat{R}_i(u) = R_i(x(u))$ and $x(u)$ is the solution of (28). For example if $R_{k^*}(y) = C_{k^*}(x_{k^*} - y)^{\alpha_{k^*}}$ then

$$x(u) = \begin{cases} x_{k^*}\left(1 - e^{-uC_{k^*}}\right) & \text{if } \alpha_{k^*} = 1, \\ x_{k^*} - \left(x_{k^*}^{1-\alpha_{k^*}} - uC_{k^*}(1-\alpha_{k^*})\right)^{\frac{1}{1-\alpha_{k^*}}} & \text{if } \alpha_{k^*} > 1. \end{cases}$$

The row vector $\hat{\varphi}(u)$ satisfies

$$\frac{d}{du}\hat{\varphi}(u) = \hat{\varphi}(u) \cdot \tilde{\mathbf{R}}_{\mathbf{k}^*}(u)\mathbf{Q},$$

where $\tilde{\mathbf{R}}_{\mathbf{k}^*}(u)$ is a diagonal matrix with diagonal elements

$$[\tilde{\mathbf{R}}_{\mathbf{k}^*}(u)]_{kk} = \begin{cases} 1 & \text{if } k = k^*, \\ \frac{\hat{R}_{k^*}(u)}{\hat{R}_k(u)} & \text{if } k \neq k^*. \end{cases}$$

According to (28) $\hat{\varphi}(0) = \varphi(0)$ and $\lim_{u\to\infty} \hat{\varphi}(u) = \lim_{x\to x_{k^*}} \varphi(x)$, from which the flux transition matrix $\mathbf{V}(0, x_{k^*})$ can be computed as $\mathbf{V}(0, x_{k^*}) = \lim_{u\to\infty} \hat{\mathbf{V}}(0, u)$, where $\hat{\mathbf{V}}(0, u)$ is the solution of

$$\frac{d}{du}\hat{\mathbf{V}}(0, u) = \hat{\mathbf{V}}(0, u)\tilde{\mathbf{R}}_{\mathbf{k}^*}(u)\mathbf{Q}, \tag{29}$$

with initial value $\hat{\mathbf{V}}(0, 0) = \mathbf{I}$. Note that the elements of $\tilde{\mathbf{R}}_{\mathbf{k}^*}(u)$ are bounded for $u \in [0, \infty)$ and vanish as u tends to infinity except $[\tilde{\mathbf{R}}_{\mathbf{k}^*}(u)]_{k^*k^*}$ which equals to one.

The same approach can be used to compute the other forward and backward flux transition matrices.

4.5 Steps of the stationary analysis

The complete analysis procedure is composed by the following steps.

i) Compute the zero transition of the fluid rate functions: $x_i, \quad i = \hat{k} + 1, \ldots, \hat{\ell}$,

ii) Compute a non singular point of each interval according to (16): $y_i, \quad i = \hat{k}, \ldots, \hat{\ell}$,

iii) Compute the forward and backward flux transition matrices based on (29): $\mathbf{V}(y_{i-1}, x_i), \mathbf{U}(y_i, x_i), \quad i = \hat{k} + 1, \ldots, \hat{\ell}$,

iv) Solve the set of linear equations (18), (25) and (26) assuming $\tilde{\varphi}_1(0) = -1$ to obtain an non-normalized solution: $\tilde{\varphi}(y_i), \quad i = \hat{k}, \ldots, \hat{\ell}$,

v) Compute the non-normalized probability masses at the boundaries by (19)-(24): $\tilde{c}(0), \tilde{c}(B)$,

vi) Compute the total probability of the non-normalized solution based on (27): C_{norm},

vii) Normalize the solution: $c(0) = \tilde{c}(0)/C_{norm}$, $c(B) = \tilde{c}(B)/C_{norm}$, $\varphi(y_i) = \tilde{\varphi}(y_i)/C_{norm}, \quad i = \hat{k}, \ldots, \hat{\ell}$,

viii) Compute the fluid density and the fluid flux at any point x based on (17) and (2): $\pi(x), \varphi(x)$.

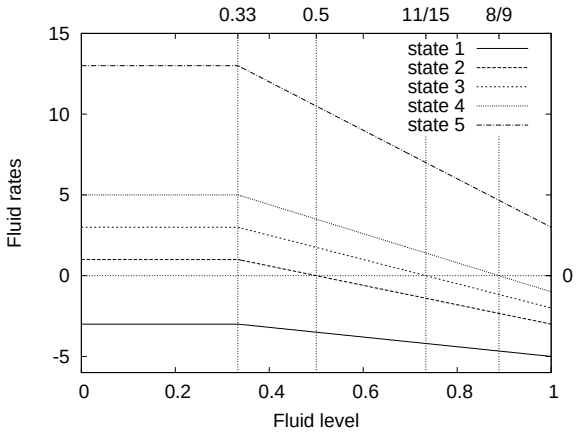

Figure 1: Fluid rates as functions of the fluid level in the example

5 Example

Let us define a fluid model with generator

$$\mathbf{Q} = \begin{bmatrix} -6 & 2 & 1 & 1 & 2 \\ 2 & -6 & 2 & 1 & 1 \\ 15 & 6 & -40 & 9 & 10 \\ 0.5 & 1.5 & 2 & -5 & 1 \\ 1 & 1 & 0 & 0 & -2 \end{bmatrix}, \tag{30}$$

and fluid rates

$$\mathbf{R}(x) = \begin{cases} \begin{bmatrix} 4 & 8 & 10 & 12 & 20 \end{bmatrix} - 7, & x \leq 1/3, \\ \begin{bmatrix} 4 & 8 & 10 & 12 & 20 \end{bmatrix} \cdot \left(\frac{5}{4} - \frac{3}{4}x\right) - 7, & x > 1/3. \end{cases} \tag{31}$$

Let the upper bound of the fluid buffer be equal to 1.

The fluid rate is negative in state 1 in $0 \leq x \leq 1$ ($\hat{k} = 1$), positive in state 5 in $0 \leq x \leq 1$ ($\hat{\ell} = 4$) and crosses the x axes in the other 3 states, at $x_2 = 1/2 = 0.5$ in state 2, at $x_3 = 11/15 \approx 0.733$ in state 3, and at $x_4 = 8/9 \approx 0.88$ in state 4. These define 4 regions with $y_1 = 0$, $y_2 = (x_2 + x_3)/2 \approx 0.6167$, $y_3 = (x_3 + x_4)/2 \approx 0.811$, $y_4 = B = 1$. The fluid rates are depicted on Figure 1.

We implemented the presented method in Matlab environment and all the experiments in this section have been made on an average PC with a dual-core CPU clocked at 3 GHz having 4 GB of RAM running a 64 bit linux system. To solve the differential equations numerically we used the Runge-Kutta method with adaptive step size and variable transformations to remove the singularities as described in Section 4.4. For

the stopping criteria a constant of 1×10^{-15} has been set, that is close to the precision of the double precision arithmetic. The computational effort is summarized in Table 1.

Operation:	Execution time:
Calculation of the forward and backward flux transition matrices:	20 sec
Solution of the flux vectors at $y_k, k = 1, \ldots, 4$ and probability masses:	0.008 sec
Calculation of the integral for normalization:	15 sec
Calculation of the pdf and cdf at 1000 points:	218 sec

Table 1: Components of the execution time of the example

The cumulative distribution function, probability flux and the density function corresponding to the different states are shown on Figure 2, 3, 4 and 5, respectively. The vertical dotted lines indicate the change of behaviour of the rate function (at $x = 1/3$) and the points where the fluid rates change sign (x_i, $i = 2, 3, 4$).

Probability mass builds up in state 1 at the lower boundary and in state 5 at the upper boundary. Probability fluxes at the boundaries are determined by (25) and (26), that leads to zero densities in states 3 and 4 at the upper boundary since $Q_{5,3} = Q_{5,4} = 0$. The probability fluxes converge to zero at the zero transitions according to Theorem 1 (Figure 3). The density functions follow different behaviors. It is bounded as in case of state 3 at x_3 ($-Q_{33}/C_3 = 40/7.5 > 1$), it is unbounded (but still integrable) in state 2 at x_2 with $-Q_{22}/C_2 = 6/6 = 1$ and in state 4 at x_4 with $-Q_{44}/C_4 = 5/9 < 1$. Figure 4 suggests that the density is "narrower" at x_2 than at x_4 as they follow different functions according to (13). This behaviour of the density can also be related with the flux curves in Figure 3. The finite density at x_2 results in the smoothest flux curve and the two different infinite density functions cause sharper and sharper flux transition from positive to negative at x_1 and x_3, respectively.

An interesting comparison can be performed between our results and the results for the case when the fluid rates depend on the fluid level in a piecewise constant way (called a multi-regime fluid queue in [11]). The regime boundaries and the rates in the various regimes are chosen such that they approximate (31) by a step function with L pieces (regimes). By denoting the upper boundary of regime k by $T^{(k)}$ and the fluid rates in regime k by $\mathbf{R}^{(k)}$ we have

$$T^{(k)} = \frac{1}{3} + \frac{2}{3}\frac{2k-1}{2L-1}, \qquad k = 1, \ldots, L, \tag{32}$$

$$\mathbf{R}^{(k)} = \begin{bmatrix} 4 & 8 & 10 & 12 & 20 \end{bmatrix} \cdot \frac{2L-k}{2L-1} - 7, \qquad k = 1, \ldots, L. \tag{33}$$

The rate functions belonging to the $L = 8$ and the $L = 30$ cases are depicted in Figures 6 and 7, respectively, and the corresponding cumulative distribution functions are plotted in Figures 8 and 9. As expected, the cdfs obtained by the two methods match quite well. In the case of $L = 8$ there is a larger difference around the zero transition in state 2 and state 4. The reason is that in the multi-regime model

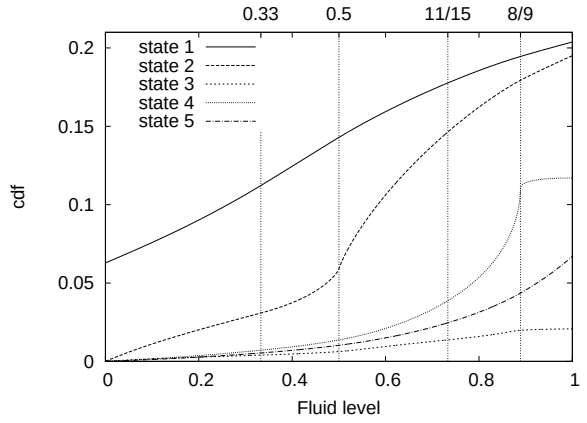

Figure 2: Cumulative distribution functions

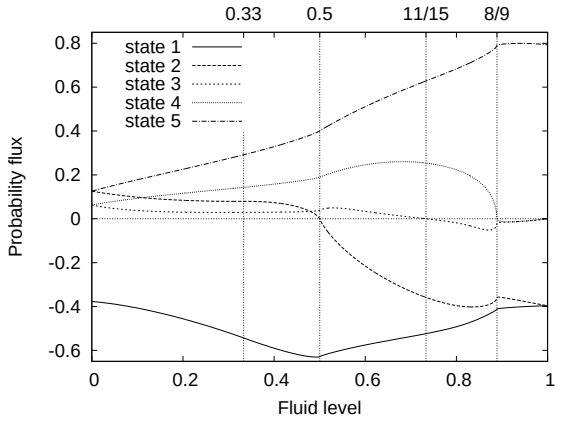

Figure 3: Probability flux x

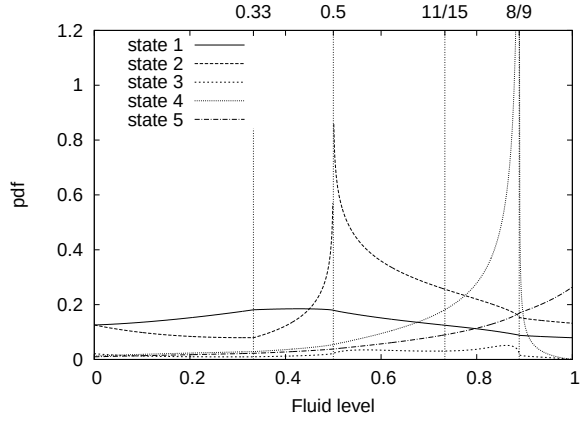

Figure 4: Probability density functions

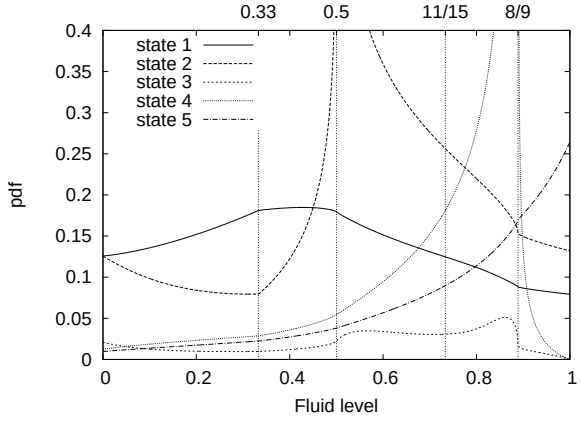

Figure 5: Probability density functions, magnified

probability mass appears at the regime boundaries where the sign of the fluid rate changes. This probability mass seems to become tangible when $-Q_{ii}/C_i \leq 1$. This happens in state 2 and state 4, resulting in a jump in the cdf, at the $T^{(k)}$ point where the sign change actually takes place, while the fluid model with continuous zero transition remains continuous around those points. This difference between the two models vanishes as L increases. At $L = 30$ it is barely noticeable in Figure 9.

Acknowledgement

S. Kolumbán was partially supported by the Hungarian National Research Fund (OTKA T68370) and the New Hungary Development Plan (Project ID: TÁMOP-4.2.1/B-09/1/KMR-2010-0002), M. Balázs by the Hungarian Scientific Research Fund (OTKA K60708, F67729), and by the Bolyai Scholarship of the Hungarian Academy of Sciences.

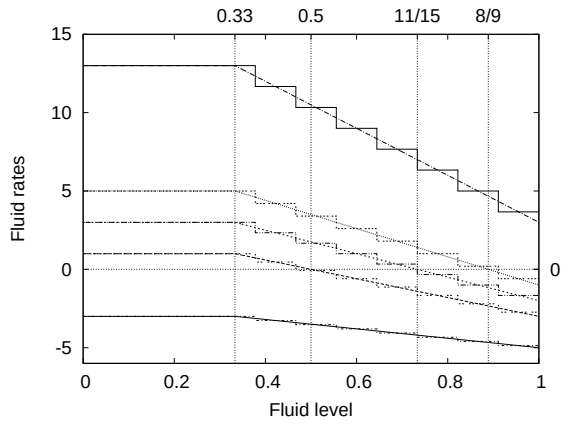

Figure 6: Piecewise constant approximation of the fluid rates with 8 steps

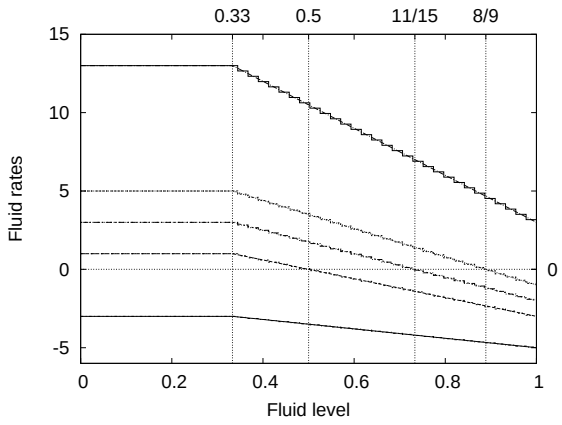

Figure 7: Piecewise constant approximation of the fluid rates with 30 steps

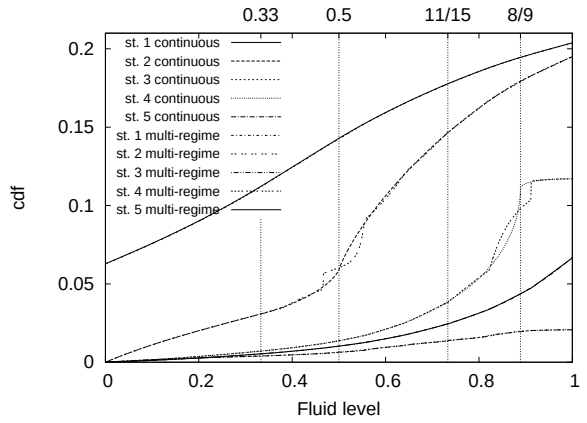

Figure 8: Piecewise constant approximation of the fluid rates with 8 steps

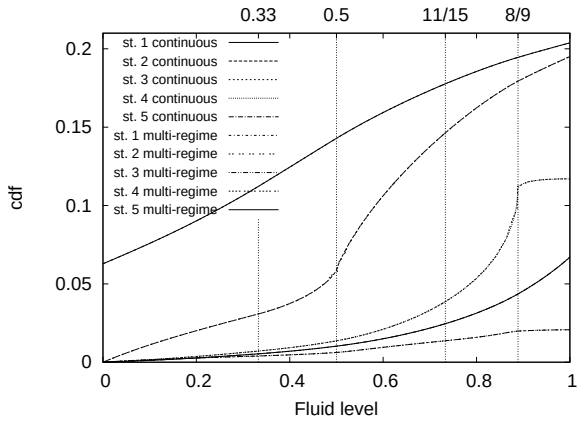

Figure 9: Piecewise constant approximation of the fluid rates with 30 steps

6 Conclusions

We investigated the stationary behaviour of Markov fluid models with continuous zero transition of the fluid rates, and showed that these models have a different qualitative behaviour at the zero transition points than the previously studied ones. If the fluid rate is bounded by finite degree polynomials of the fluid level in an environment of the zero transition then there is no probability mass developing in this environment. We also classified the cases when the fluid density is finite or unbounded.

We proposed and implemented a numerical procedure to evaluate the considered set of Markov fluid models. Finally a numerical example indicates convincing coincidence with the theoretical results and with the results of an approximate (piecewise constant) numerical analysis approach.

References

[1] Ivo Adan and Jacques Resing. A two-level traffic shaper for an on-off source. *Performance Evalutation*, 42:279–298, 2000.

[2] Soohan Ahn and V. Ramaswami. Fluid flow models and queues–a connection by stochastic coupling. *Stochastic Models*, 19:325–348, 2003.

[3] Andrei Badescu, Lothar Breuer, Ana Da Silva Soares, Guy Latouches, Marie-Ange Remiche, and David Stanford. Risk processes analyzed as fluid queues. *Scand. Actuar. J.*, 2005(2):127–141, 2005.

[4] N.G. Bean, M.M. O'Reilly, and J.E. Sargison. A stochastic fluid flow model of the operation and maintenance of power generation systems. *IEEE Tr. on Power Systems*, 25(3):1361 –1374, 2010.

[5] O. Boxma, H. Kaspi, O. Kella, and D. Perry. On/off storage systems with state-dependent input, output, and switching rates. *Probability in the Engineering and Informational Sciences*, 19:1–14, 2005.

[6] Ana da Silva Soares and Guy Latouche. Matrix-analytic methods for fluid queues with finite buffers. *Performance Evaluation*, 63(4-5):295 – 314, 2006.

[7] Ana da Silva Soares and Guy Latouche. Fluid queues with level dependent evolution. *European Journal of Operational Research*, 196(3):1041 – 1048, 2009.

[8] A. I. Elwalid and D. Mitra. Statistical multiplexing with loss priorities in rate-based congestion control of high-speed networks. *IEEE Transaction on communications*, 42(11):2989–3002, Nov. 1994.

[9] M. Gribaudo and M. Telek. Stationary analysis of fluid level dependent bounded fluid models. *Performance Evaluation*, 65:241–261, 2008.

[10] G. Horton, V. Kulkarni, D. Nicol, and K. Trivedi. Fluid stochastic petri nets: Theory, applications, and solution techniques. *European Journal of Operational Research*, 105:184–201, 1998.

[11] H.E. Kankaya and N. Akar. Solving multi-regime feedback fluid queues. *Stochastic Models*, 24(3):425–450, 2008.

[12] H.E. Kankaya and N. Akar. Exact analysis of single-wavelength optical buffers with feedback markov fluid queues. *Optical Communications and Networking, IEEE/OSA Journal of*, 1(6):530 –542, 2009.

[13] V. G. Kulkarni. Fluid models for single buffer systems. In J. H. Dshalalow, editor, *Models and Applications in Science and Engineering*, Frontiers in Queueing, pages 321–338. CRC Press, 1997.

[14] W. Scheinhardt, van N. Foreest, and M.R.H. Mandjes. Continuous feedback fluid queues. *Operations Research Letters*, 33:551–559, 2005.

[15] K. Sohraby and N. Akar. Infinite/finite buffer markov fluid queues: A unified analysis. *Journal of Applied Probability*, 41(2):557–569, 2004.